JOURNAL OF VIROLOGY, Dec. 2005, p. 14719–14729 Vol. 79, No. 23
0022-538X/05/$08.00+0 doi:10.1128/JVI.79.23.14719–14729.2005

The Conserved Poxvirus L3 Virion Protein Is Required for Transcription of Vaccinia Virus Early Genes

Wolfgang Resch and Bernard Moss*

Laboratory of Viral Diseases, National Institute of Allergy and Infectious Diseases, National Institutes of Health, Bethesda, Maryland 20892

Received 24 April 2005/Accepted 7 September 2005

We provide the initial characterization of the product of the vaccinia virus L3L open reading frame (VACWR090), which is conserved in all sequenced members of the poxvirus family. The predicted polypeptide contains no motifs or other features that provided a clue to the role of the L3 protein, and no functional information was available regarding a homolog discovered in *Plasmodium falciparum*. The L3 protein was expressed following viral DNA replication, a finding consistent with a putative late promoter sequence, and was packaged as a non-membrane protein in mature virus particles. A recombinant virus, in which the L3L gene was regulated by the *Escherichia coli lac* operator/repressor system, had a conditional lethal phenotype. The virus replicated in the presence of inducer, but in its absence, the yields of infectious virus were reduced by 99%. When cells were infected without inducer, however, no defect in gene expression or morphogenesis was noted. Virus particles lacking L3, which assembled in the absence of inducer, were indistinguishable from wild-type virions with regard to morphology, major structural proteins, and DNA content but were noninfectious. L3-deficient virions were able to bind and penetrate cells but produced extremely small amounts of viral early mRNA. A defect in transcription was demonstrated by in vitro studies with permeabilized virions, but soluble extracts of L3-deficient virions showed normal levels of template-dependent transcriptional activity, indicating that only transcription of the packaged genome is impaired.

The poxvirus family is comprised of viruses with large, linear, double-stranded DNA genomes that replicate exclusively in the cytoplasm (21). Vaccinia virus (VACV), the most thoroughly studied member of the family, encodes approximately 200 proteins with roles in host defense, viral transcription, genome replication, and the formation of progeny virus particles (13, 22). Approximately 90 predicted proteins are shared by all vertebrate poxviruses, and at least 49 of these are encoded by insect poxviruses as well (30). Although these highly conserved proteins are likely to have essential functions, many have not yet been characterized. One such universally conserved protein, encoded by the VACWR090 (L3L) open reading frame (ORF) of the Western Reserve (WR) strain of VACV, has no recognizable motif or non-poxvirus homolog with known function. (Note that commonly used names for VACV ORFs are based on their location within a HindIII fragment, followed by a L or R indicating left or right direction of transcription, respectively; the latter can be omitted when referring to the protein product of the gene). To investigate the role of the predicted L3 protein, we have taken a reverse genetic approach and constructed a recombinant VACV in which the L3 ORF is stringently regulated by the *Escherichia lac* operator/repressor system (3). Here, we present the initial characterization of the L3 protein and demonstrate that it is a virion component. Virions lacking the L3 protein appeared morphologically normal but had greatly reduced infectivity due to an early postentry block manifested as a reduction in early gene expression. A defect in transcription of the packaged genome but not exogenous template was demonstrated by in vitro studies.

* Corresponding author. Mailing address: Laboratory of Viral Diseases, National Institutes of Health, 4 Center Dr., MSC 0445, Bethesda, MD 20892-0445. Phone: (301) 496-9869. Fax: (301) 480-1147. E-mail: bmoss@nih.gov.

MATERIALS AND METHODS

Cells and virus strains. BS-C-1 cells were maintained in minimum essential medium with Earle's salts supplemented with 2.5% fetal bovine serum, 100 units/ml of penicillin, and 100 μg/ml of streptomycin. HeLa and baby hamster kidney (BHK) cells were maintained in Dulbecco's modified Eagle's medium supplemented with 10% fetal bovine serum and antibiotics as described above. The WR strain and the recombinant vT7lacOI VACV were propagated as described previously (3). vL3Li was propagated in the presence of 25 μM isopropyl-β-D-thiogalactopyranoside (IPTG). Intracellular mature virion (IMV) particles of the WR and vL3Li strains produced in the presence or absence of IPTG were purified by sucrose gradient centrifugation as described previously (12). Particle concentration was determined by light scattering as optical density at 260 nm (OD_{260}) $\times$ 1.2 $\times$ 10^{10} particles/ml (12).

Antibodies. Rabbit antisera were raised against a peptide derived from the predicted L3 sequence (amino acids 45 to 59, KPRLQPNQPPKQDNK) and one peptide from the A3 sequence (P4b/4b; amino acids 632 to 643, QYISARHITELF) plus a C-terminal cysteine required for coupling to keyhole limpet hemocyanin (Covance Research Products). Anti-A14-C (5), anti-A17-N (5), anti-A6/Rpo19 (2), and anti-H4/Rap94 (1) rabbit antisera, as well as anti-B5 rat monoclonal antibody 19C2 (25) were described previously. S. Shuman (Sloan-Kettering Institute, New York, N.Y.) kindly provided anti-H6/topoisomerase and anti-J6/Rpo147 rabbit antisera. Polyclonal anti-A4 antiserum (11) was provided by M. Esteban (Centro Nacional de Biotecnologia, Madrid, Spain) and murine monoclonal anti-L1 antibody 7D11 (15) was provided by A. Schmaljohn (United States Army Medical Research Institute of Infectious Diseases, Fort Detrick, MD).

Plasmid and recombinant VACV construction. To construct pVOTE-L3L, the L3L ORF was amplified by PCR from genomic DNA using oligonucleotide primers 5′-ATA AAT TCC ATA TGA ATA CCC GTA CCG ATG TTA C-3′ (NdeI site underlined) and 5′-TTA AAT AAT TTT AAT TCG TTT AAC GAA TAT CTT G-3′, and the PCR product was cloned into the NdeI-SmaI sites of pVOTE.2 downstream of an encephalomyocarditis virus leader sequence (32). This plasmid was used to introduce the inducible copy of L3L into the A56R (hemagglutinin) locus of vT7lacOI by homologous recombination using mycophenolic acid selection as described previously (32), resulting in the intermediate virus vL3L/L3Li. The inducible L3L copy was verified by PCR amplification and sequence analysis. The endogenous L3L ORF was replaced with the enhanced green fluorescent protein (GFP) marker gene using homologous recombination with a linear DNA fragment containing the GFP sequence flanked by partial sequences of the L2R and L4R ORFs. This construct preserved the first 36

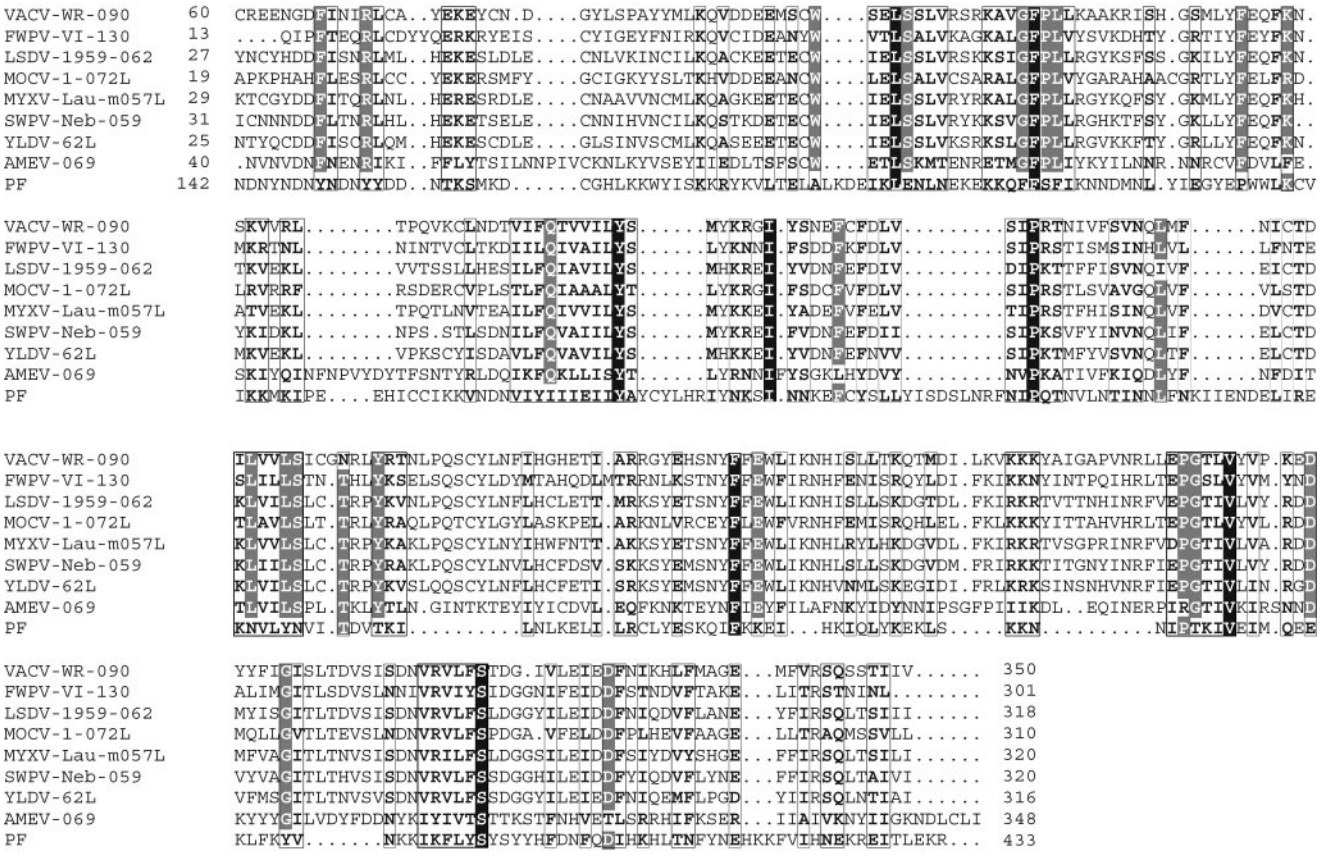

FIG. 1. Multiple-sequence alignment of L3 orthologs. The nonredundant protein sequence database (National Center for Biotechnology Information) was searched using the BLASTP program to identify putative homologs (4). A multiple-sequence alignment was constructed with the T-Coffee algorithm (23). The alignment includes one representative amino acid sequence from each genus of *Poxviridae* and one sequence from *Plasmodium falciparum* strain 3D7. Amino acids at invariant positions are shown as white letters on black background. Amino acids at positions that are invariant in all but one sequence are shown as white letters against gray background. Other conserved amino acids are shown in bold type and boxed. Position numbers are indicated for each sequence at the beginning and the end of the aligned fragment. Abbreviations: VACV, vaccinia virus (*Chordopoxvirinae*); FWPV, fowlpox virus (*Avipoxvirinae*); LSDV, lumpy skin disease virus (*Capripoxvirinae*); MOCV, molluscum contagiosum (*Molluscipoxvirinae*); MYXV, myxoma virus (*Leporipoxvirinae*); SWPV, swinepox virus (*Suipoxvirinae*); YLDV, Yaba-like disease virus (*Yatapoxvirinae*); AMEV, Amsacta moorei entomopoxvirus (*Entomopoxvirinae* B); PF, *Plasmodium falciparum* (accession code NP_704661). The virus strain and ORF designation are also indicated after the virus.

nucleotides of the L3L ORF, which function as a promoter for L4R but eliminated the start codon of L3L as well as a second methionine codon. This fragment was generated in three steps. First, two independent PCRs were carried out to amplify the flanking regions. The upstream flanking region (containing part of L2R) was amplified with oligonucleotide primers 5′-TTA TAA TAT TGG CAG CGT TGT TTA TGT ACT A-3′ and 5′-GTC TAc TgC agT cAc Aaa ATA AAG TAA TAA AAA AT-3′ (PstI site underlined; lowercase nucleotides indicate mutations introduced to create the PstI site and remove identical nucleotides between the L2R-L3R overlap and the inducible L3R). The downstream flanking region (containing part of the L4R sequence) was amplified using oligonucleotide primers 5′-TTT GTC TAg ATT ATC GTT TGT AAa ATC GGT ACG GGT ATT aAT T-3′ (XbaI site underlined; lowercase letters indicated mutations introduced to create the XbaI site and remove possible start codons from the L3L fragment not deleted to preserve the L4R promoter) and 5′-GTA TAC TCA GTC GAC GCG GAT TCC ATA TTT TCT TTA TA-3′. In the second step, the PCR-amplified fragments were digested with the indicated restriction enzymes, mixed with a fragment containing the GFP ORF and the F18L late promoter obtained by digesting plasmid p11GFP (unpublished data) with XbaI and PstI, and ligated together. The third step consisted of PCR amplification with the outmost primers using the ligation reaction product as the template. The final PCR product was transfected into cells infected with vL3L/L3Li at 0.5 PFU per cell using Lipofectamine 2000 (Invitrogen). Recombinant viruses expressing GFP were isolated by five rounds of plaque purification using an inverted fluorescence microscope. The correct site of recombination was verified by PCR analysis and sequencing.

Electron microscopy. For transmission electron microscopy, BS-C-1 cells were grown in 60-mm-diameter dishes and infected with 3 PFU of vL3Li per cell in the presence or absence of 25 μM IPTG. At 20 h after infection, cells were fixed and prepared for transmission electron microscopy as described previously (9). Purified IMVs were adsorbed to carbon-coated Formvar grids and negatively stained with 7% uranyl acetate in 50% ethanol.

Confocal microscopy. BHK cells were infected with 2 PFU of vL3Li per cell in the presence or absence of 25 μM IPTG. At 24 h after infection, cells were fixed with 4% paraformaldehyde for 10 min, blocked for 30 min with 3% bovine serum albumin, washed three times with phosphate-buffered saline, and incubated with rat anti-B5 followed by Cy5-coupled anti-rat antibody (Jackson Immunoresearch). After three more washes, cells were permeabilized with 0.2% Triton X-100 in phosphate-buffered saline, and actin and DNA were visualized with phalloidin coupled to Alexa Fluor 568 (Molecular Probes) and diamidino-2-phenylindole (Molecular Probes), respectively. HeLa cells used for the IMV entry assay were stained as described previously (28). Images were collected with a Leica TCS-NT/SP2 inverted confocal microscope system.

Southern slot blot analysis. Serial dilutions of equal numbers of L3-containing (L3+) and L3-deficient (L3−) particles were adjusted to 0.4 M NaOH and 10 mM EDTA in a final volume of 100 μl and heated to 100°C for 10 min to disrupt virions and denature the packaged DNA. Heated samples were filtered

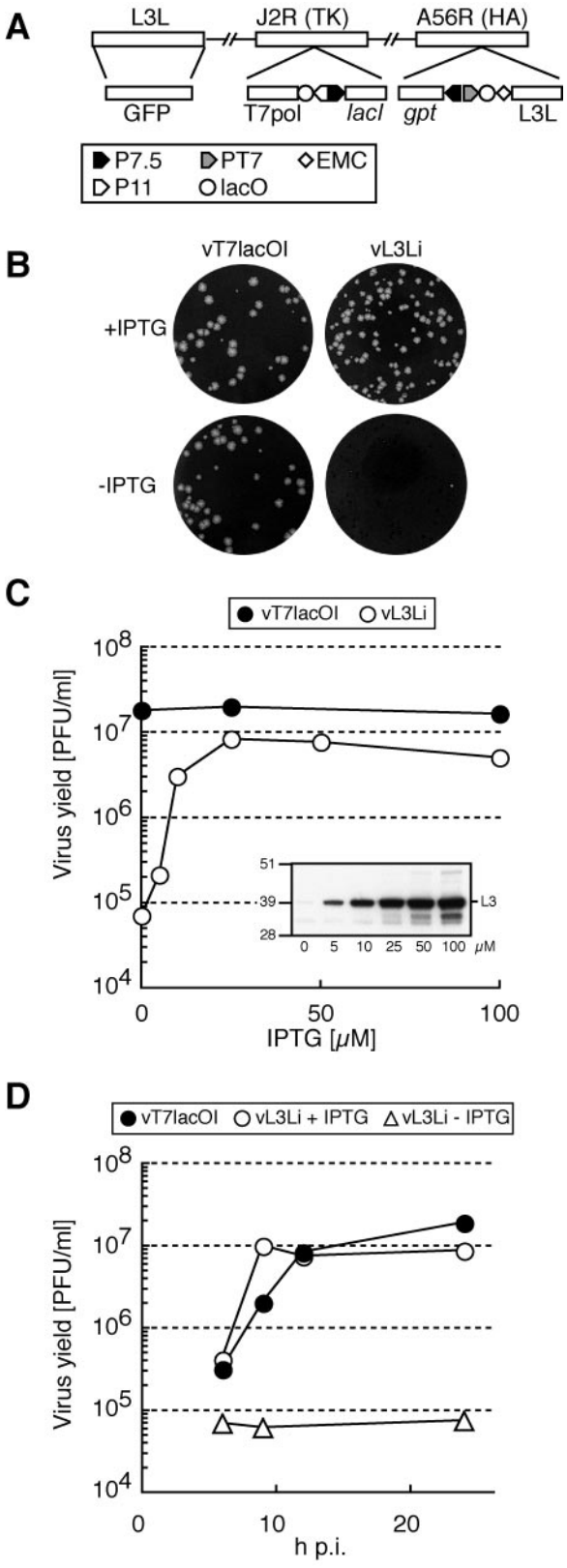

FIG. 2. Construction and characterization of a recombinant VACV with an inducible L3L ORF (vL3Li). (A) Genome structure of vL3Li. Three loci at which vL3Li differs from the WR strain are shown: L3L, J2R (thymidine kinase [TK]), and A56R (hemagglutinin [HA]). Below the loci are schematics of the modifications. Abbreviations: T7pol, bacteriophage T7 RNA polymerase gene; lacO, *lac* operator; P11, a VACV late promoter; P7.5, a VACV early/late promoter; *lacI*, *E. coli lac* repressor gene; *gpt*, *E. coli* guanine phosphoribosyltransferase gene; PT7, bacteriophage T7 promoter; EMC, encephalomyocarditis virus cap-independent translation enhancer element. (B) Plaque phenotype of vL3Li. BS-C-1 cells were infected with vL3Li and vT7lacOI in the absence (+) or presence (−) of 25 μM IPTG. After 48 h, cells were fixed and stained with crystal violet. (C) Dependence of vL3Li replication on IPTG. BS-C-1 cells were infected with 10 PFU per cell of vT7lacOI or with vL3Li in the presence of 0 to 100 μM IPTG, and viral yield was determined after 24 h by plaque assay in the presence of 25 μM IPTG. The insert shows a Western blot of whole-cell extracts prepared from vL3Li-infected cells at the indicated IPTG concentrations. (D) One-step growth curve of vL3Li. BS-C-1 cells were infected with 10 PFU per cell of vT7lacOI or vL3Li in the absence or presence of 25 μM IPTG, and virus yield was determined from 2 to 48 h postinfection (h p.i.).

through a positively charged nylon membrane in a slot blot apparatus (Schleicher & Schuell). Wells were rinsed once with 0.4 M NaOH before the membrane was neutralized with 2× SSC (1× SSC is 0.15 M NaCl [pH 7] plus 0.015 M sodium citrate), and the DNA was covalently cross-linked to the membrane by UV irradiation. Membranes were incubated in hybridization buffer (0.09 M sodium citrate, pH 7, 0.9 M NaCl, 0.1% Ficoll, 0.1% polyvinylpyrrolidone, 0.1% bovine serum albumin, 0.5% sodium dodecyl sulfate [SDS]) for 1 h at 68°C. A heat-denatured E9L DNA fragment labeled with ^{32}P using random priming (Decaprime II; Ambion) was added directly to the prehybridization reaction mixture to a final concentration of 1×10^6 cpm/ml, and incubation was continued for 15 h. Membranes were washed with increasing stringency, and hybridized, radioactively labeled DNA was detected by autoradiography and quantified by storage phosphor autoradiography with a Typhoon 8600 (Molecular Dynamics).

Northern blot analysis. Total RNA was prepared from infected cells with the RNeasy mini kit (QIAGEN). Equal amounts of total RNA were denatured by glyoxylation and separated on 1% agarose gels. Equal loading was confirmed by analysis of ethidium bromide-stained rRNA bands. RNA was transferred to a positively charged nylon membrane by downward capillary transfer in 20 mM NaOH. Detection and quantitation were carried out as described above for "Southern slot blot analysis."

Transcription by VACV cores. Purified virions were incubated in a final volume of 20 μl containing 50 mM Tris HCl (pH 8.0), 5 mM dithiothreitol (DTT), 10 mM $MgCl_2$, 0.05% Nonidet P-40 (NP-40), 5 mM ATP, 1 mM GTP, 1 mM CTP, 0.02 mM UTP, and 1 μCi of [α-^{32}P]UTP (3,000 Ci/mmol) for 1 h at 30°C. Incorporation of ^{32}P into trichloroacetic acid-insoluble material was determined by scintillation counting. Kinetic experiments were carried out under the same conditions using 0.25 OD_{260} unit of virions per reaction. At the indicated time, a 30-μl aliquot was withdrawn and cooled and EDTA was added to a final concentration of 30 mM. Cores were collected by centrifugation at 20,000 × *g* for 20 min in the cold. Methylation of RNA caps was measured by incorporation of ^3H from [^3H]methyl-*S*-adenosylmethionine in the presence of 1 mM UTP.

Preparation and analysis of virion extracts. Virion extracts were prepared as described previously (24) from 10 OD_{260} units of virions. Transcription reaction mixtures contained 50 ng of pSB24 (20) plasmid DNA linearized with SmaI, 15 mM Tris, pH 8.0, 2 mM DTT, 2 mM ATP, 1 mM CTP, 20 μM UTP, 100 μM 3′-*O*-methyl GTP, 5 μCi [α-^{32}P]UTP, 5 mM $MgCl_2$, and 0.5 μl virion extract or DEAE column fraction in a total volume of 10 μl. Reaction mixtures were incubated at 30°C for 1 h before the amount of [α-^{32}P]UMP incorporated into trichloroacetic acid-insoluble material was determined by scintillation counting. The pSB24 plasmid was generated by Steven Broyles (Purdue University) and contains a synthetic early promoter upstream of a 382-nucleotide G-less cassette. RNA products were isolated from larger reaction mixture volumes using the pooled peak fractions by phenol-chloroform extraction and isopropanol precipitation.

RESULTS

The L3L ORF encodes a highly conserved, essential viral protein. The L3L ORF (VACWR090) is predicted to encode a 40.6-kDa protein without notable functional sequence motifs. Orthologs of this ORF were found in all poxvirus genomes

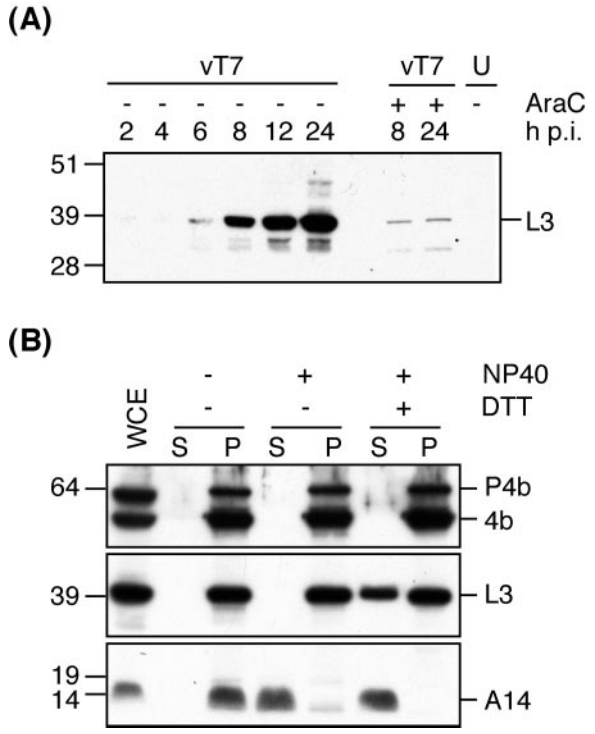

FIG. 3. Synthesis and IMV packaging of L3. (A) L3 expression kinetics. BS-C-1 cells were infected with 10 PFU per cell of vT7lacOI, and whole-cell extracts were prepared at the indicated times (hours postinfection [h p.i.]). Extracts from uninfected cells (U) and cells infected in the presence of cytosine arabinoside (AraC) were also prepared; extracts were analyzed by SDS-PAGE and Western blotting with antiserum to L3 as described previously (20). The positions and masses (in kilodaltons) of marker proteins are indicated on the left. (B) L3 is packaged into IMVs. Sucrose gradient-purified IMVs were extracted with NP-40 or NP-40 plus DTT or mock treated and separated into soluble (S) and pellet (P) fractions. Proteins in both fractions were separated by SDS-PAGE followed by Western blotting with anti-P4b, anti-L3, or anti-A14 sera. The positions and masses (in kilodaltons) of marker proteins are indicated on the left. WCE, whole-cell extracts.

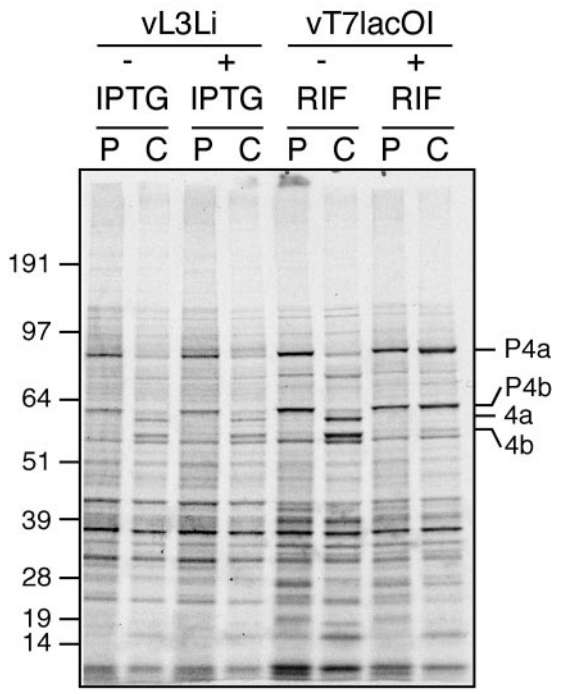

FIG. 4. Synthesis and processing of viral late proteins. BS-C-1 cells were infected with 4 PFU per cell of vL3Li in the absence (−) or presence (+) of 25 μM IPTG or with 4 PFU per cell of vT7lacOI in the presence (+) or absence (−) of 100 μg/ml rifampin (RIF). Infected cells were pulse-labeled with 100 μCi of [^{35}S]methionine and [^{35}S]cysteine per ml for 30 min at 9 h postinfection, and whole-cell lysates were prepared either immediately (pulse [P]) or after a further 15-h incubation in the presence of excess unlabeled methionine and cysteine (chase [C]). Proteins were separated by SDS-PAGE and visualized by autoradiography. The migration positions and masses (in kilodaltons) of marker proteins are indicated on the left. The positions of major core protein precursors P4a and P4b as well as their proteolytically processed mature forms 4a and 4b are indicated on the right.

sequenced to date. A multiple-sequence alignment of orthologs from representative members of each genus of the *Poxviridae* family is shown in Fig. 1. The amino termini are less well conserved than the remainder of the proteins in this family and could not be aligned. In addition, a predicted homolog of unknown function was discovered in the published genome of *Plasmodium falciparum* during a BLAST search (Fig. 1).

To determine whether L3L encodes an essential protein, we generated a recombinant VACV (vL3Li) in which L3 synthesis was dependent on the presence of IPTG. vL3Li was constructed in two steps. First, an inducible copy of the L3L ORF was inserted into the hemagglutinin locus of vT7lacOI (32), a recombinant VACV expressing an IPTG-inducible T7 RNA polymerase (Fig. 2A). In the second step, the endogenous L3L ORF of the intermediate virus was replaced with the GFP marker gene by homologous recombination (Fig. 2A). vL3Li produced plaques of greatly reduced size in the absence of IPTG compared to those produced in the presence of 25 μM IPTG (Fig. 2B), suggesting that L3L is essential for efficient viral replication. In the presence of IPTG, vL3Li plaques were slightly smaller than plaques produced by the parental vT7lacOI VACV strain (Fig. 2B). Virus yield under single-cycle conditions was reduced approximately 99% in the absence of IPTG (Fig. 2C and D). The yield increased with IPTG concentrations up to 25 μM, whereas L3 levels continued to increase up to 100 μM IPTG (Fig. 2C). Nevertheless, at the optimal IPTG concentration, the yield of vL3Li was less than that of the parental strain, a finding consistent with the difference in plaque size. At 25 μM, the kinetics of virus production under single-cycle conditions were similar for vL3Li and vT7lacOI (Fig. 2D).

The L3 protein is expressed late and packaged into virions. Analysis of the sequence upstream of the L3L ORF revealed a putative late promoter (10). To determine whether L3 was indeed synthesized with late kinetics, whole-cell extracts of VACV-infected cells were analyzed by SDS-polyacrylamide gel electrophoresis (PAGE) and Western blotting with a rabbit antiserum raised against amino acids 45 to 59 of L3. A protein of approximately 40 kDa was detected 6 h after infection and continued to increase for up to 24 h (Fig. 3A). Suppression of VACV DNA replication with cytosine arabinoside (AraC) inhibited L3 expression (Fig. 3A). Timing of expression and dependence on DNA replication suggested that L3 belongs to the late class of proteins. However, a small amount of L3

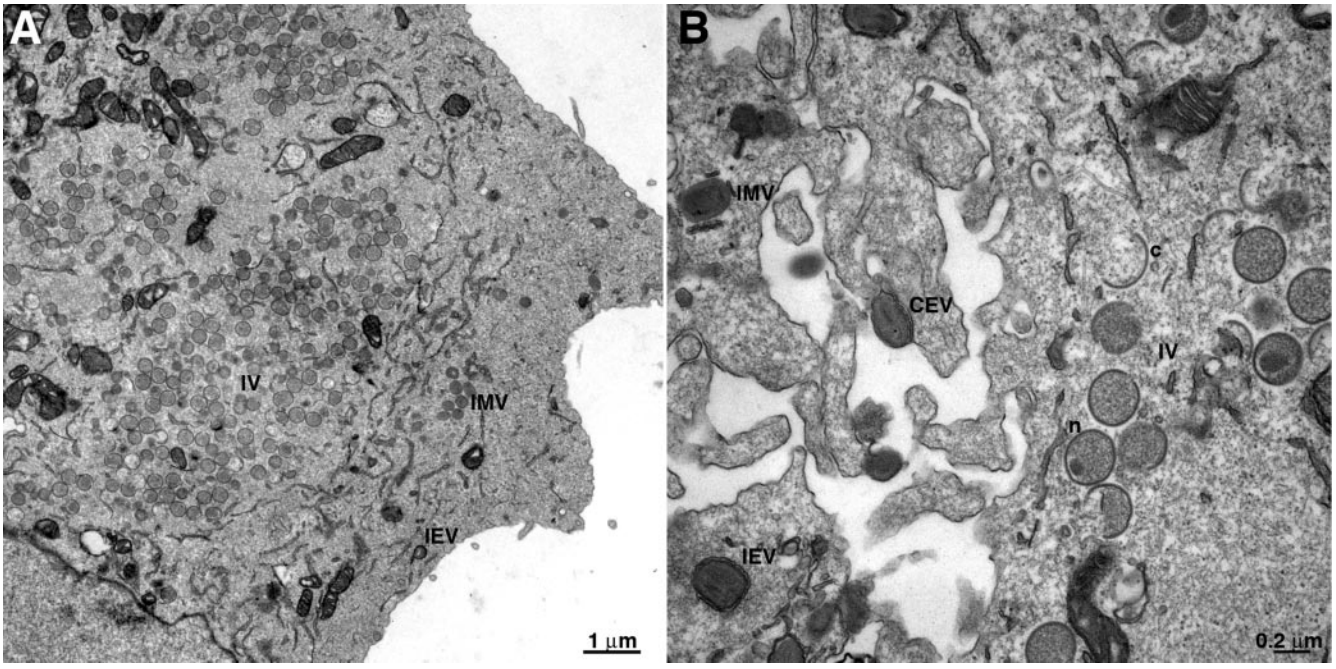

FIG. 5. Electron microscopy of infected cells. BS-C-1 cells were infected with 3 PFU per cell of vL3Li in the absence of IPTG. Cells were fixed and prepared for transmission electron microscopy at 20 h after infection. Lower (A) and higher (B) magnification electron micrographs are shown with their scale indicated by bars. Abbreviations: c, crescent; IV, immature virion; n, nucleoid within an IV; IMV, intracellular mature virion; IEV, intracellular enveloped virion; CEV, cell-associated enveloped virion.

was detected at 2 h after infection as well as at later times in the presence of cytosine arabinoside. This small amount of L3 might have been packaged into the virions used in the infection.

The L3 protein was detected by Western blotting of proteins from sucrose gradient-purified intracellular mature virions. However, to be certain that this did not represent the detection of trace amounts by a sensitive assay, we made a blot of proteins from whole-cell infected cell lysates and purified IMV. We then probed the same blot with antibody to L3 and antibody to bona fide virion components 4b and A14. The relative amounts of L3 in lysates compared to those of L3 in IMVs were similar to the relative amounts of 4b and A14 in lysates compared to those of 4b and A14 in IMVs (Fig. 3B). These data suggest that L3 was specifically incorporated into virions. The nonionic detergent NP-40 alone was unable to extract any L3 from purified virions but did completely extract the membrane protein A14 (Fig. 3B). NP-40 in combination with DTT partially solubilized L3 from virions but did not extract the core structural protein P4b/4b (Fig. 3B). Together with the absence of a predicted membrane-spanning helix, our results suggested that L3 is a loosely packaged internal virion protein.

VACV late proteins are synthesized and processed normally. VACV gene expression occurs as an ordered synthesis of early, intermediate, and late proteins. Concomitantly, host protein synthesis is reduced, allowing abundant late viral proteins to be selectively labeled with radioactive amino acids. Viral protein synthesis was analyzed by pulse-labeling BS-C-1 cells infected with vL3Li in the presence or absence of 25 μM IPTG. Whole-cell extracts of labeled cells were subjected to SDS-PAGE and autoradiography. As shown in Fig. 4, the pattern of viral protein synthesis 9 h after infection was similar in cells infected with the parental vT7lacOI and vL3Li with or without IPTG.

The normal pattern of viral proteins suggested that early steps in the replicative cycle were not dependent on synthesis of L3. (Note, however, that vL3Li stocks were made in the presence of IPTG, and therefore, the virus inoculum contained L3.) To determine whether virion maturation was proceeding normally in the absence of L3 synthesis, we analyzed the proteolytic processing of core proteins, a signature event in the transition from immature to mature virus particles (17). To this end, pulse-labeled cells were shifted to chase medium with excess unlabeled methionine and cysteine for a further 15 h before analysis. For a control, vT7lacOI infections were also carried out in the presence of rifampin, an inhibitor of morphogenesis and protein processing (17). Normal processing of the core proteins was observed regardless of the absence of IPTG (Fig. 4), suggesting that L3 was not required for maturation of virus particles.

L3 is not required for formation of intracellular or extracellular virions. To directly examine the effect of L3 repression on the stage of virus assembly, thin sections of cells infected with vL3Li in the absence of IPTG were examined by transmission electron microscopy (Fig. 5). All stages of morphogenesis, including immature virions, IMVs, intracellular enveloped virions, and extracellular cell-associated enveloped virions (CEVs), were observed and were indistinguishable in morphology from those seen in the presence of IPTG (data not shown), a finding consistent with the apparently normal processing of core proteins.

Confocal microscopy experiments were carried out to determine whether actin tails were associated with the CEVs formed in

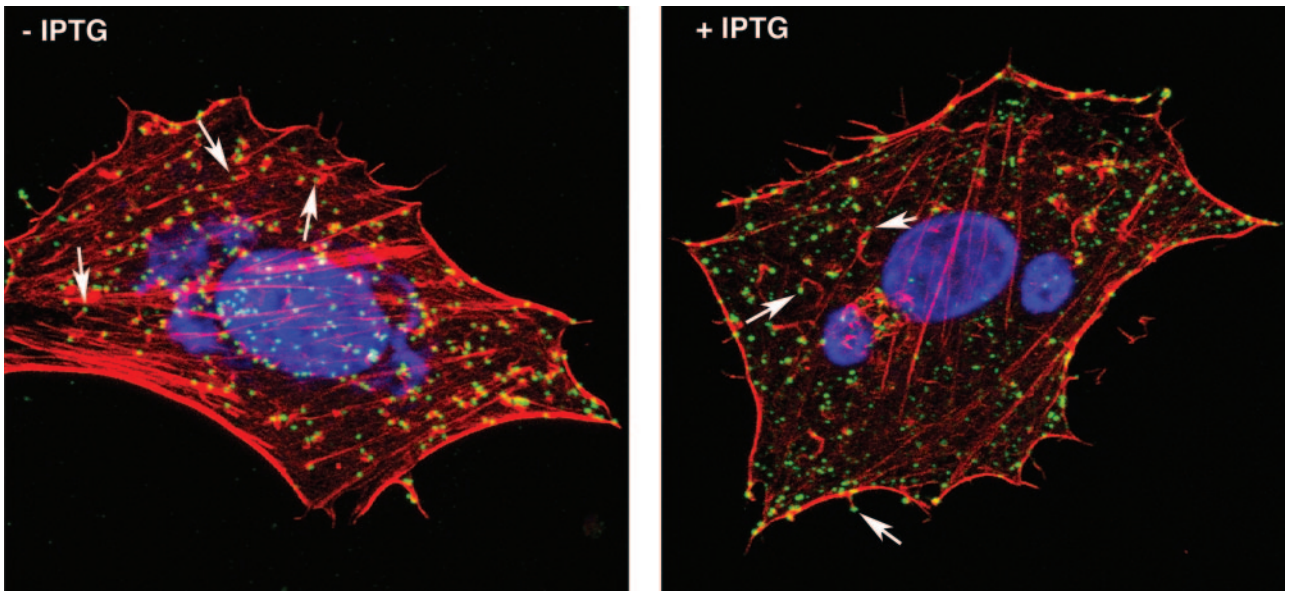

FIG. 6. Detection of CEVs and actin tails by confocal microscopy. BHK cells were infected with 2 PFU per cell of vL3Li in the absence (−) or presence (+) of 25 μM IPTG. After 24 h, cells were fixed and CEVs were visualized by staining with anti-B5 monoclonal antibody, followed by Cy5-conjugated goat anti-rat antibody (green). Cells were then washed and permeabilized prior to staining filamentous actin with Alexa Fluor 568 coupled to phalloidin (red) and staining DNA with diamino-2-phenylindole dihydrochloride (blue). White arrows point to examples of CEVs at the tips of actin tails. Images are representative of the larger populations and are shown as maximum-intensity projections calculated from stacks of optical sections obtained by confocal microscopy.

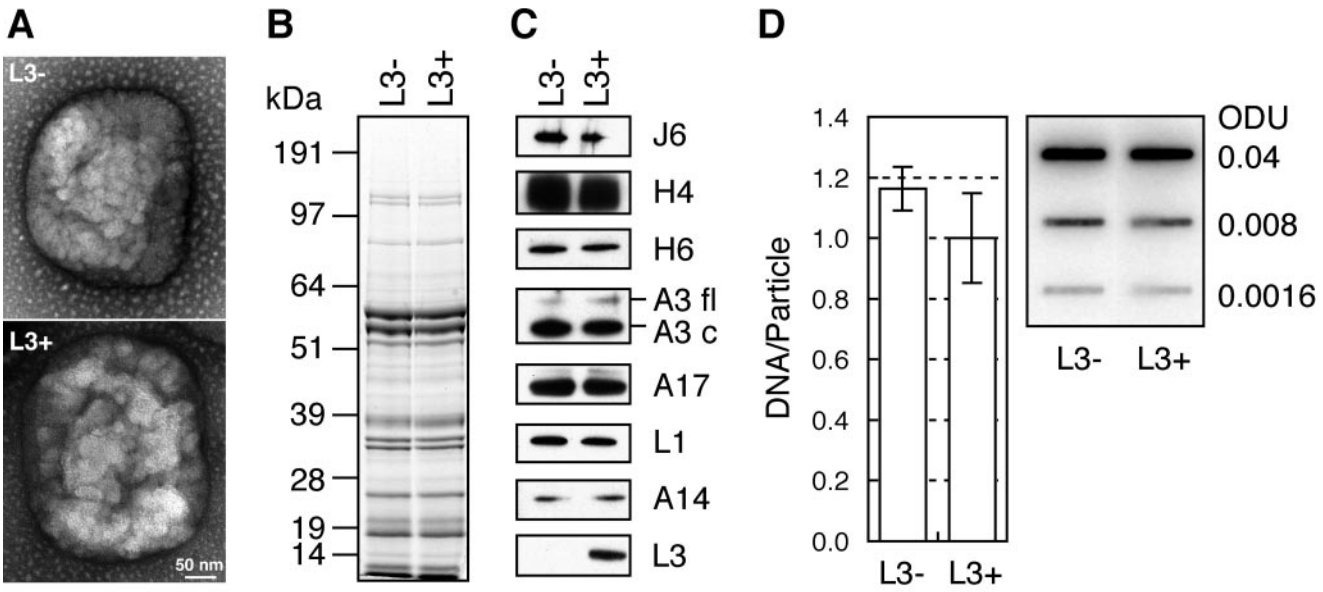

FIG. 7. Morphology and protein and DNA contents of L3+ and L3− IMVs. (A) Morphology. vL3Li IMVs produced in the absence (L3−) and presence (L3+) of IPTG were purified by sucrose gradient centrifugation, adsorbed to grids, washed, and negatively stained. Electron micrographs of representative particles are shown with a scale bar. (B) Polypeptide composition of purified virions. Proteins from 0.14 OD_{260} unit of purified L3+ and L3− virions were separated by SDS-PAGE and stained with colloidal Coomassie blue. The migration positions and masses (in kilodaltons) of marker proteins are indicated on the left. (C) Immunoblots of purified virions. Proteins from 0.01 OD_{260} unit of purified L3+ and L3− virions were separated by SDS-PAGE and transferred to nitrocellulose membranes, and the indicated core and membrane proteins were detected immunologically. A composite of the bands is shown. The antibodies used were as follows: anti-J6, RNA polymerase subunit Rpo147; anti-H4, RNA polymerase-associated protein; anti-H6, topoisomerase; anti-A3, structural protein 4b and its precursor P4b; anti-A17, IMV membrane protein; anti-L1, IMV membrane protein; anti-A14, IMV membrane protein. (D) DNA content of purified virions. (Right) The indicated amounts (ODU, OD_{260} unit) of purified virions were disrupted; the DNA contained in the virions was denatured and adsorbed to a nylon membrane. VACV DNA was detected by annealing a radioactively labeled VACV DNA fragment. The graph shows DNA content per particle normalized to the content in the L3+ virions.

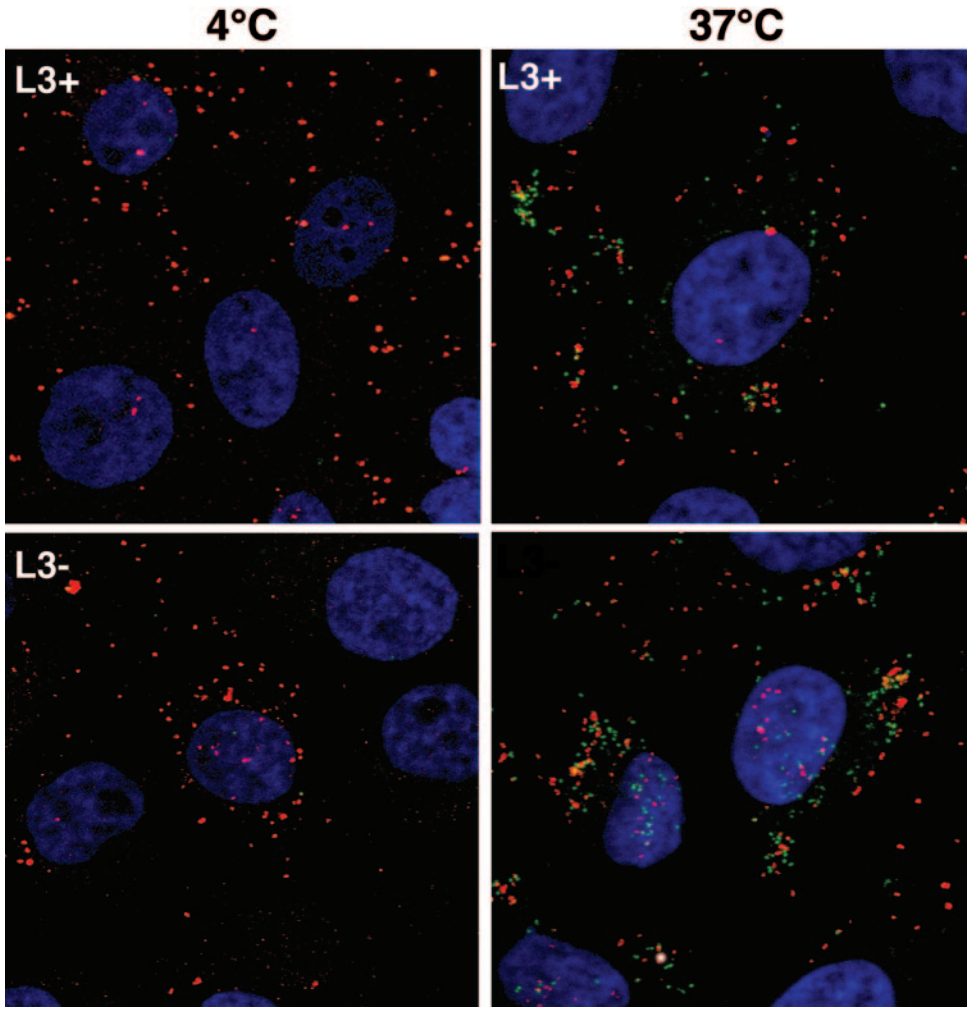

FIG. 8. Binding and penetration of purified virions into cells. Equal numbers of purified L3+ and L3− virions were allowed to adsorb to HeLa cells for 1 h at 4°C and then either fixed immediately or fixed after further incubation at 37°C for 2 h. Cells were washed, permeabilized, and sequentially stained with mouse monoclonal anti-L1 antibody and rabbit anti-A4 sera. The primary antibodies were detected with Alexa Fluor 594-coupled goat anti-mouse antibody (red) and Alexa Fluor 488-coupled goat anti-rabbit antibody (green), respectively. DNA was stained with diamino-2-phenylindole (blue). Stacks of optical sections were obtained by confocal microscopy, and representative images are shown here as maximum-intensity projections.

the absence of IPTG, a step required for efficient cell-to-cell spread. Cells were infected with vL3Li in the presence or absence of IPTG, and CEVs were visualized on unpermeabilized cells using a monoclonal antibody against the external domain of the B5 protein component of the CEV envelope. After staining with B5, cells were permeabilized and actin was visualized by staining with a fluorescently labeled phalloidin derivative. CEVs were detected on the surfaces of infected cells irrespective of the presence or absence of IPTG (Fig. 6). Furthermore, the absence of IPTG did not inhibit the formation of actin tails with CEVs at their tip.

IMVs lacking L3 have normal morphology and protein and DNA contents but have reduced infectivity compared to IMVs containing L3. The inability to form infectious progeny under single-cycle conditions in the absence of IPTG, despite the normal processing of core proteins, and the apparently normal numbers and appearance of virus particle assembly intermediates suggested that virions lacking L3 had significantly reduced infectivity. In all previous experiments, virions produced in the presence of IPTG and therefore containing L3 were used to infect cells. To determine the infectivity of IMVs lacking L3, cells were infected with vL3Li in the presence or absence of IPTG and purified by sucrose gradient centrifugation. The appearance and position of the particles in the gradient and the overall particle yields were similar under both conditions. The specific infectivity of L3− IMVs, determined as the PFU-to-particle ratio (PFUs determined in the presence of IPTG), however, was on average 50-fold less than that of L3+ IMVs in three independent preparations.

Negatively stained IMVs from the L3+ and L3− preparations had indistinguishable morphologies (Fig. 7A). In addition, when proteins from equal numbers of particles of both preparations were separated by SDS-PAGE and visualized by Coomassie blue staining, no significant differences in the major protein bands were apparent (Fig. 7B). The presence of several specific enzymatic, structural, and membrane proteins was con-

firmed by preparing immunoblots (Fig. 7C). Again, no differences between the preparations were apparent other than the expected absence of L3 from IMVs produced without IPTG. Furthermore, similar amounts of viral DNA were detected on slot blots prepared from equal amounts of L3− and L3+ IMV (Fig. 7D). The association of the viral DNA with the particles was confirmed by cesium chloride density gradient centrifugation (data not shown).

IMVs lacking the L3 protein can enter cells. Since L3 did not appear to be an IMV membrane protein, we expected L3− IMV to adhere to and penetrate cells normally. To confirm this supposition, we used an assay based on the ability of antibodies to certain core proteins to react with cores liberated into the cytoplasm after entry, but not with membrane-enclosed cores on the surfaces of cells even after fixation and permeabilization (19, 31). Equal numbers of L3+ and L3− particles were allowed to bind to BS-C-1 cells for 1 h at 4°C. Cells were then washed and either fixed immediately or after incubation for an additional 1 h at 37°C to allow entry of adsorbed IMVs into the cells. To detect particles on the cell surface and cores in the cytoplasm, we used antibodies to the L1 membrane protein and the A4 core protein, respectively. After incubation at 4°C, both L3+ and L3− IMV particles attached to cells were detected by their punctate staining with L1 antibody, but no cores were detected with A4 antibody (Fig. 8). Upon raising the temperature to 37°C, which allows virus entry, cores were detected in the cytoplasm of cells infected with L3− and L3+ IMVs, in addition to residual intact IMVs on the cell surface (Fig. 8). Note that particles staining with A4 antibody do not colocalize with particles staining with L1 antibody, as the membrane is removed during the entry process. In contrast, cores are not detected when IMVs lacking either the A28 or H2 entry/fusion proteins are analyzed under the same conditions (22, 24). Thus, the entry of IMV is not dependent on the presence of L3.

Early RNA is reduced in cells infected with IMVs lacking the L3 protein compared to cells infected with IMVs containing L3. Soon after entry into cells, viral cores transcribe early genes because all of the necessary enzymes and factors are packaged. To test whether this process occurs normally with L3− IMVs, cells were infected with an equal number of L3+ and L3− particles, corresponding to 10 PFU/cell of the L3+ virus preparation. After 2 h, total RNA was extracted from infected cells and analyzed by Northern blotting using probes against three early RNA species. In each case, the amount of viral RNA detected was greatly reduced in infections with the L3− virus compared with infections with the L3+ virus (Fig. 9A). This reduction could be caused by either a decrease or delay in early transcription. We distinguished between these possibilities by allowing infections to proceed for up to 6 h in the presence of the DNA synthesis inhibitor AraC. Under these conditions, C11R RNA increased only slightly from 1% of the wild-type level at 2 h after infection to 4% at 6 h in L3− virus-infected cells, whereas L3+ virus-infected cells transcribed wild-type virus-like amounts of RNA (Fig. 9B). These results suggested an early postentry defect resulting in a profound reduction in the synthesis or stability of viral RNA. We did note, however, that all cells showed a cytopathic effect after 6 h, a finding that suggested low-level expression of viral proteins.

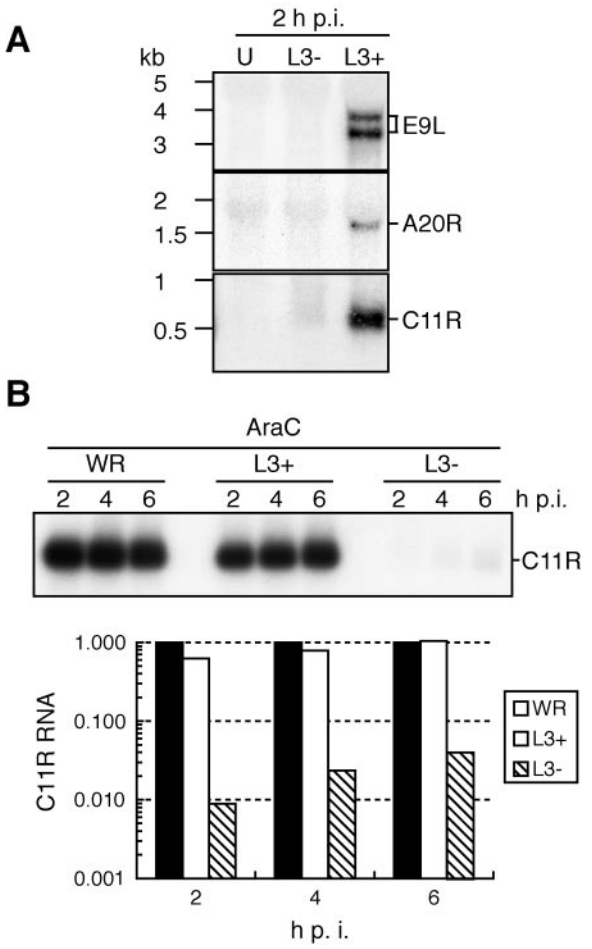

FIG. 9. Early gene expression. (A) Analysis of three viral early RNAs in cells infected with purified L3+ and L3− virions. BS-C-1 cells were mock infected (uninfected [U]) or infected with 10 PFU per cell of L3+ virions or with an equal number of L3− virions. At 2 h postinfection (p.i.), total RNA was extracted, glyoxylated, and resolved by agarose gel electrophoresis. RNA was then transferred to a nylon filter, and transcripts were detected with radioactively labeled DNA fragments obtained by PCR amplification of E9L (DNA polymerase), A20R (DNA polymerase processivity factor), and C11R (VACV growth factor) sequences. The positions and lengths (in kilobases) of RNA size markers are indicated on the left. (B) Accumulation of an early RNA. BS-C-1 cells were treated with 40 μg/ml of cytosine arabinoside (AraC) for 1 h before infection with 10 PFU per cell of purified L3+ virions or with equal numbers of purified L3− or WR virions. Infected cells were maintained in the presence of AraC for the indicated times before isolation of total RNA. C11R RNA levels were determined by Northern blot analysis as described above for panel A. The RNA was quantified with a phosphorimager and plotted on a logarithmic scale.

L3− virions produce less RNA in vitro than L3+ virions do. The failure to detect accumulation of viral RNA in infected cells could occur because of impaired transcription or enhanced RNA degradation. Since IMVs contain the complete VACV transcription machinery, we tested whether L3− virions were impaired in transcription in vitro. To this end, purified L3+ and L3− virions were permeabilized and incubated with ribonucleoside triphosphates, and incorporation of [α-^{32}P]UTP into trichloroacetic acid-insoluble material was determined. In each case, RNA

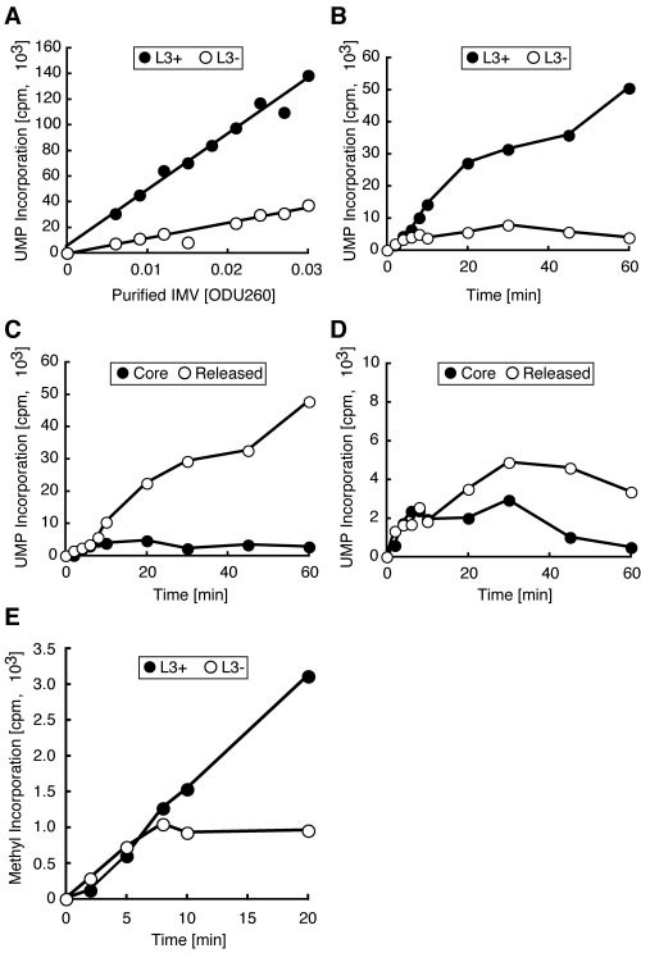

FIG. 10. RNA synthesis and release by permeabilized virions. (A) In vitro transcription by different numbers of permeabilized virions. Sucrose gradient-purified L3+ or L3− IMVs were permeabilized with nonionic detergent and incubated with [α-^{32}P]UTP and other unlabeled ribonucleoside triphosphates for 30 min. Incorporation of [α-^{32}P]UMP into trichloroacetic acid-precipitable material was determined by scintillation counting. Lines are best-fit regressions with slopes of 4×10^6 and 1×10^6 for L3+ and L3− IMVs, respectively. ODU260, OD_{260} unit. (B to D) Kinetic analysis of transcription by permeabilized virions. Aliquots were withdrawn from transcription reaction mixtures and analyzed as described above for panel A (B) or separated into core-associated and released RNA fractions for L3+ (C) and L3− (D) virions. Note the different scales in panels C and D. (E) Cap methylation by permeabilized virions. Transcription reactions were carried out as described above for panel A except for the inclusion of the methyl donor [^{3}H]methyl-*S*-adenosylmethionine and the omission of radioactively labeled UTP.

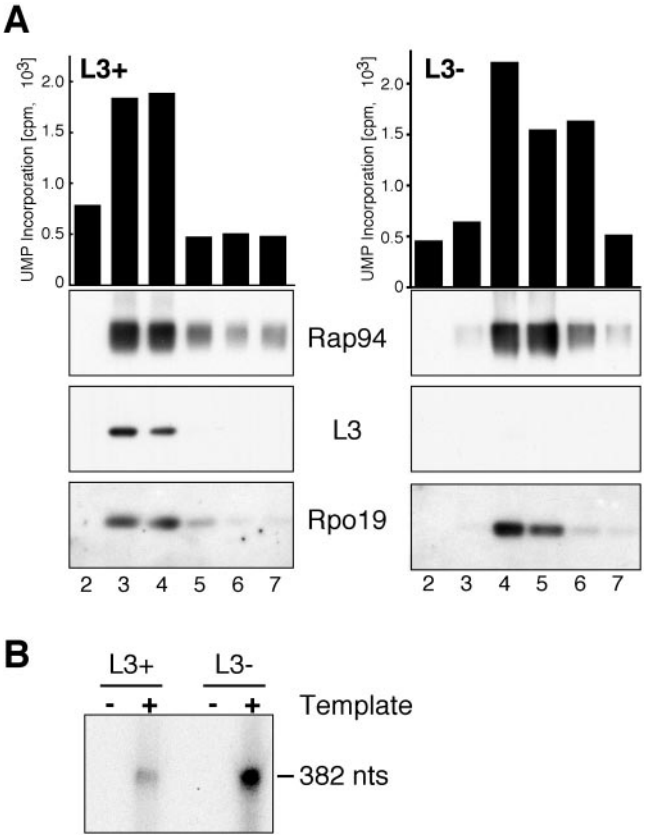

FIG. 11. Promoter-dependent transcription by mutant virion extracts. (A) Components of the transcription machinery were solubilized from L3+ and L3− IMVs with deoxycholate and separated from endogenous genomes by DEAE chromatography. Fractions were collected, and template-dependent transcription activity was measured by UMP incorporation. In addition, the presence of Rap94 and Rpo19, both components of the early promoter-specific RNA polymerase holoenzyme, as well as L3 were analyzed by SDS-PAGE followed by immunoblotting. Results are shown for DEAE fractions 2 to 7. (B) RNA product size. RNA transcripts were purified from transcription reactions carried out with the peak activity fractions of the DEAE column and separated on a 4% denaturing polyacrylamide gel. Reactions were carried out in the presence (+) or absence (−) of template with L3+ or L3− virus extracts. nts, nucleotides.

synthesis was proportionate to virus added, but there was a fourfold difference in transcription between the two viruses (Fig. 10A). Kinetic experiments suggested that the rate of transcription by L3− virions decreased over time, leading to a bigger difference in total transcript levels at later times (Fig. 10B). In addition, the fraction of transcripts released from cores was higher in reaction mixtures containing L3+ virions (Fig. 10C) than in those containing L3− virions (Fig. 10D). The lengths of RNAs produced in the presence and absence of L3 were similar, although small pattern differences were noted (data not shown).

VACV virions contain a capping enzyme that creates the methyl-7-GpppN cap cotranscriptionally using *S*-adenosylmethionine as the methyl donor. To determine whether RNA synthesized by L3− particles was capped, transcription reactions were carried out in the presence of [^{3}H]methyl-*S*-adenosylmethionine, and the incorporation of ^{3}H into trichloroacetic acid-insoluble material was determined. Initial rates of methyl incorporation by L3− and L3+ virions were similar (Fig. 10E), suggesting that there was no capping defect per se. However, there was a sharp decrease in the rate of methyl incorporation after the initial phase. This could be due to a reduction in transcription initiation or a reduction in capping. However, the reduction in [α-^{32}P]UTP incorporation is consistent with inhibition of transcription initiation.

L3 is not required for template-dependent transcription activity by IMV extracts. The reduced transcription activity of

permeabilized L3− virions despite the apparent presence of a normal complement of transcription enzymes raised the question of whether L3 was required for template-dependent transcription per se or whether L3 was required only for transcription within cores. To address this issue, equal numbers of L3− and L3+ virions were solubilized with deoxycholate and endogenous nucleic acid was removed by DEAE-cellulose chromatography. Fractions eluting from the DEAE column contained similar amounts of transcription factors as exemplified by the RNA polymerase-associated protein Rap94, which is required for early transcription, and the RNA polymerase subunit Rpo19 (Fig. 11A), irrespective of the presence of L3. Fractions from both extracts were able to transcribe a linear duplex DNA substrate containing an early promoter at comparable levels (Fig. 11A), and the sizes of the transcribed products were identical to each other (Fig. 11B) and to RNA made by a soluble extract of WR virions (not shown). No transcription was detected in the absence of template.

Some factors such as capping enzyme are tightly associated with the RNA polymerase holoenzyme. This does not seem to be the case for L3, as we were unable to detect this protein by immunoblotting (data not shown) of a preparation of RNA polymerase purified as described previously (16). However, we cannot exclude the possibility of transient interactions during transcription.

DISCUSSION

The function of the L3 protein, which is encoded by one of the approximately 50 genes that are conserved in all poxvirus genomes (30), could not be predicted, since sequence analysis did not reveal any recognizable motifs. Although we identified a homolog of L3 in *Plasmodium falciparum*, there were no reports of its expression or function. We demonstrated that L3 is synthesized late in the virus replication cycle as a protein of approximately 40 kDa, in agreement with its predicted mass and putative promoter sequence. L3 was localized in the viral factory (data not shown) and was packaged into mature virions. A nonionic detergent was unable to extract L3 from the virus particle, suggesting that it is an internal protein, a finding consistent with the absence of a predicted membrane-spanning domain. However, the ability of the detergent together with a reducing agent to partially extract L3 distinguished it from some core proteins with structural roles, such as 4b encoded by the A3L gene.

To investigate the function of L3, a mutant in which L3 expression was dependent on the presence of IPTG was constructed. In the absence of inducer, the mutant virus was unable to spread or produce infectious progeny, indicating that L3L is an essential gene. Virus stocks prepared in the presence of IPTG were used to infect cells in the presence or absence of the inducer. The pattern of late protein synthesis was normal, and proteolytic processing of core proteins occurred irrespective of the presence of IPTG, suggesting that the L3 protein is unnecessary for morphogenesis. This was confirmed by examination of transmission electron microscopic images of infected cells, which showed immature and mature virus particles. Furthermore, the cell-associated enveloped virions formed in the absence of IPTG were associated with actin tails, which are important for cell-to-cell spread. Virions assembled in the absence of IPTG and therefore lacking L3 were purified and found to be indistinguishable in electron microscopic appearance, complement of major proteins, and DNA content from virions made in the presence of IPTG and containing L3. The presence of several specific structural, membrane, and enzymatic proteins was confirmed by immunoblotting. In particular, several examined components of the VACV transcription machinery, which is packaged into virions, were present in unchanged amounts. Nevertheless, L3− virions had only 2% of the specific infectivity of L3+ virions.

Several conditionally lethal mutant VACVs that produce virions with normal appearance and DNA content have been described elsewhere (8, 14, 18, 27, 29, 33, 34). Such mutants have defects in virus entry (26, 27) or early transcription (8, 14, 18, 29, 33, 34). Since the proteins required for entry are membrane proteins, we anticipated correctly that purified L3− virions would adhere to and enter cells with an efficiency comparable to that of L3+ virions. Instead, cells infected with purified L3− virions contained very little viral early RNA compared to cells infected with equal numbers of L3+ particles. Early transcription is carried out in the cytoplasm within VACV cores, which contain packaged DNA and the necessary proteins. Nascent RNAs are believed to be extruded from the intact cores. The reduced amounts of early transcripts in vivo could therefore be explained either by reduced transcriptional activity of viral cores or by a more rapid turnover of extruded RNAs. We measured the transcriptional activity of L3+ and L3− viral cores directly by permeabilizing IMVs in vitro under reducing conditions and found that the absence of L3 results in an up to 10-fold reduction of transcriptional activity, indicating that inhibition of transcription is the likely explanation for the very low early RNA levels in vivo. The RNA produced by L3− virions was also released to a lesser extent, but the length of the RNA appeared to be similar to that synthesized by L3+ virions. The rate of transcription fell over time for L3− virions, but not for L3+ virions. The rate of RNA capping by L3− IMVs was markedly reduced after initially proceeding at a rate comparable to that of L3+ virions. Since RNA contains only one cap, which is at the 5′ end, the rapid drop in capping activity could be due to a reduction in transcription initiation or to a sudden decrease in capping of transcripts. The decrease of UTP incorporation, which occurs slightly later than the decrease in capping, is consistent with an overall reduction of transcription initiations, maybe after the first round of RNA synthesis.

Approximately 20 IMV proteins are known to be involved in transcription or RNA modification, including the eight subunits of the RNA polymerase, an RNA polymerase-associated protein, the early transcription factor, the capping enzyme, the poly(A) polymerase, two helicases, a single-stranded nucleic acid binding protein, a topoisomerase, and a phosphatase (6). Suppression of some of these proteins results in defects during morphogenesis, whereas others are dispensable for the formation of normal-appearing IMVs. Since early transcription has been reconstituted with purified components (7) and we could not detect L3 in a purified RNA polymerase preparation, it seemed unlikely that L3 was required for transcription of naked templates. Indeed, the normal template-dependent transcription activity of soluble L3-deficient virion extracts con-

firmed that L3 was required for transcription only within the confines of the intact core. In this regard, the absence of L3 causes a defect similar to that produced by the absence of the H6 topoisomerase (8), the I8 nucleoside triphosphate phosphohydrolase II (14), the H1 phosphatase (18), or the L4 DNA/RNA binding protein (33). While the mechanism of L3 action remains to be determined, one can hypothesize that L3 may contribute to functions that are required for the transcription of topologically constrained, chromatin-like templates, such as promoter unwinding, maintenance of single-stranded DNA, or regulation of supercoiling.

ACKNOWLEDGMENTS

We thank A. Weisberg for electron microscopy and N. Cooper for providing virus stocks and cells. M. Esteban, S. Shuman, and A. Schmaljohn graciously provided antibodies and antisera.

This research was supported by the intramural research program of the NIAID, NIH.

REFERENCES

1. **Ahn, B.-Y., and B. Moss.** 1992. RNA polymerase-associated transcription specificity factor encoded by vaccinia virus. Proc. Natl. Acad. Sci. USA **89:**3536–3540.
2. **Ahn, B.-Y., J. Rosel, N. B. Cole, and B. Moss.** 1992. Identification and expression of *rpo19*, a vaccinia virus gene encoding a 19-kilodalton DNA-dependent RNA polymerase subunit. J. Virol. **66:**971–982.
3. **Alexander, W. A., B. Moss, and T. R. Fuerst.** 1992. Regulated expression of foreign genes in vaccinia virus under the control of bacteriophage T7 RNA polymerase and the *Escherichia coli lac* repressor. J. Virol. **66:**2934–2942.
4. **Altschul, S. F., W. Gish, W. Miller, E. W. Myers, and D. J. Lipman.** 1990. Basic local alignment search tool. J. Mol. Biol. **215:**403–410.
5. **Betakova, T., E. J. Wolffe, and B. Moss.** 1999. Regulation of vaccinia virus morphogenesis: phosphorylation of the A14L and A17L membrane proteins and C-terminal truncation of the A17L protein are dependent on the F10L protein kinase. J. Virol. **73:**3534–3543.
6. **Broyles, S. S.** 2003. Vaccinia virus transcription. J. Gen. Virol. **84:**2293–2303.
7. **Broyles, S. S., L. Yuen, S. Shuman, and B. Moss.** 1988. Purification of a factor required for transcription of vaccinia virus early genes. J. Biol. Chem. **263:**10754–10760.
8. **Da Fonseca, F., and B. Moss.** 2003. Poxvirus DNA topoisomerase knockout mutant exhibits decreased infectivity associated with reduced early transcription. Proc. Natl. Acad. Sci. USA **100:**11291–11296.
9. **da Fonseca, F. G., E. J. Wolffe, A. Weisberg, and B. Moss.** 2000. Effects of deletion or stringent repression of the H3L envelope gene on vaccinia virus replication. J. Virol. **74:**7518–7528.
10. **Davison, A. J., and B. Moss.** 1989. The structure of vaccinia virus late promoters. J. Mol. Biol. **210:**771–784.
11. **Demkowicz, W. E., J. S. Maa, and M. Esteban.** 1992. Identification and characterization of vaccinia virus genes encoding proteins that are highly antigenic in animals and are immunodominant in vaccinated humans. J. Virol. **66:**386–398.
12. **Earl, P. L., B. Moss, L. S. Wyatt, and M. W. Carroll.** 1998. Generation of recombinant vaccinia viruses, p. 16.17.1–16.17.19. *In* F. M. Ausubel, R. Brent, R. E. Kingston, D. D. Moore, J. G. Seidman, J. A. Smith, and K. Struhl (ed.), Current protocols in molecular biology, vol. 2. Greene Publishing Associates & Wiley Interscience, New York, N.Y.
13. **Goebel, S. J., G. P. Johnson, M. E. Perkus, S. W. Davis, J. P. Winslow, and E. Paoletti.** 1990. The complete DNA sequence of vaccinia virus. Virology **179:**247–266, 517–563.
14. **Gross, C. H., and S. Shuman.** 1996. Vaccinia virions lacking the RNA helicase nucleoside triphosphate hydrolase II are defective in early transcription. J. Virol. **70:**8549–8570.
15. **Hooper, J. W., D. M. Custer, C. S. Schmaljohn, and A. L. Schmaljohn.** 2000. DNA vaccination with vaccinia virus L1R and A33R genes protects mice against a lethal poxvirus challenge. Virology **266:**329–339.
16. **Katsafanas, G. C., and B. Moss.** 1999. Histidine codons appended to the gene encoding the RP022 subunit of vaccinia virus RNA polymerase facilitate the isolation and purification of functional enzyme and associated proteins from virus-infected cells. Virology **258:**469–479.
17. **Katz, E., and B. Moss.** 1970. Formation of a vaccinia virus structural polypeptide from a higher molecular weight precursor: inhibition by rifampicin. Proc. Natl. Acad. Sci. USA **6:**677–684.
18. **Liu, K., B. Lemon, and P. Traktman.** 1995. The dual-specificity phosphatase encoded by vaccinia virus, VH1, is essential for viral transcription in vivo and in vitro. J. Virol. **69:**7823–7834.
19. **Locker, J. K., A. Kuehn, S. Schleich, G. Rutter, H. Hohenberg, R. Wepf, and G. Griffiths.** 2000. Entry of the two infectious forms of vaccinia virus at the plasma membrane is signaling-dependent for the IMV but not the EEV. Mol. Biol. Cell **11:**2497–2511.
20. **Luo, Y., J. Hagler, and S. Shuman.** 1991. Discrete functional stages of vaccinia virus early transcription during a single round of RNA synthesis *in vitro*. J. Biol. Chem. **266:**13303–13310.
21. **Moss, B.** 2001. *Poxviridae*: the viruses and their replication, p. 2849–2883. *In* D. M. Knipe and P. M. Howley (ed.), Fields virology, 4th ed., vol. 2. Lippincott Williams & Wilkins, Philadelphia, Pa.
22. **Moss, B., and T. G. Senkevich.** 2002. Orthopoxvirus, p. 885–901. *In* C. A. Tidona and G. Darai (ed.), The Springer index of viruses. Springer-Verlag, Berlin, Germany.
23. **Notredame, C., D. G. Higgins, and J. Heringa.** 2000. T-Coffee: a novel method for fast and accurate multiple sequence alignment. J. Mol. Biol. **302:**205–217.
24. **Rohrmann, G., and B. Moss.** 1985. Transcription of vaccinia virus early genes by a template-dependent soluble extract of purified virions. J. Virol. **56:**349–355.
25. **Schmelz, M., B. Sodeik, M. Ericsson, E. J. Wolffe, H. Shida, G. Hiller, and G. Griffiths.** 1994. Assembly of vaccinia virus: the second wrapping cisterna is derived from the trans Golgi network. J. Virol. **68:**130–147.
26. **Senkevich, T. G., and B. Moss.** 2005. Vaccinia virus h2 protein is an essential component of a complex involved in virus entry and cell-cell fusion. J. Virol. **79:**4744–4754.
27. **Senkevich, T. G., B. M. Ward, and B. Moss.** 2004. Vaccinia virus A28L gene encodes an essential protein component of the virion membrane with intramolecular disulfide bonds formed by the viral cytoplasmic redox pathway. J. Virol. **78:**2348–2356.
28. **Senkevich, T. G., B. M. Ward, and B. Moss.** 2004. Vaccinia virus entry into cells is dependent on a virion surface protein encoded by the A28L gene. J. Virol. **78:**2357–2366.
29. **Simpson, D. A., and R. C. Condit.** 1994. The vaccinia virus A18R protein plays a role in viral transcription during both the early and late phases of infection. J. Virol. **68:**3642–3649.
30. **Upton, C., S. Slack, A. L. Hunter, A. Ehlers, and R. L. Roper.** 2003. Poxvirus orthologous clusters: toward defining the minimum essential poxvirus genome. J. Virol. **77:**7590–7600.
31. **Vanderplasschen, A., M. Hollinshead, and G. L. Smith.** 1998. Intracellular and extracellular vaccinia virions enter cells by different mechanisms. J. Gen. Virol. **79:**877–887.
32. **Ward, G. A., C. K. Stover, B. Moss, and T. R. Fuerst.** 1995. Stringent chemical and thermal regulation of recombinant gene expression by vaccinia virus vectors in mammalian cells. Proc. Natl. Acad. Sci. USA **92:**6773–6777.
33. **Wilcock, D., and G. L. Smith.** 1996. Vaccinia virions lacking core protein VP8 are deficient in early transcription. J. Virol. **70:**934–943.
34. **Zhang, Y., B.-Y. Ahn, and B. Moss.** 1994. Targeting of a multicomponent transcription apparatus into assembling vaccinia virus particles requires RAP94, an RNA polymerase-associated protein. J. Virol. **68:**1360–1370.